

# Advances in Zr-Based Alloys

Quan Dong and Jun Tan \* 

College of Materials Science and Engineering, Chongqing University, Chongqing 400044, China; q.dong@cqu.edu.cn

\* Correspondence: jun.tan@cqu.edu.cn

Due to outstanding mechanical properties [1–4], good anti-neutron irradiation resistance [5–9], superior corrosion resistance properties [10–13], good biocompatibility [14–16], and so forth, zirconium (Zr) and its alloys have important application potential in the fields of nuclear technologies, aerospace, chemical research, biomedical industries, etc. [17]. However, as the needs of various industries continue to change, higher performance requirements have been put forward for Zr alloys. Therefore, advanced high-performance Zr alloys need to be designed, developed, and optimized to meet this demand.

An improved understanding of related research fields can be quickly obtained using bibliometric analyses [18–20]. To conduct an analysis of the research status on Zr alloys, relevant papers pertaining to Zr alloys published in the last 10 years were retrieved using the Web of Science Core Collection. The search employed Zirconium alloy as its subject term. A total of 6268 papers were identified, selected, and subsequently downloaded for in-depth analysis. Utilizing the retrieved data, Figure 1 presents an analysis of the quantity of publications about Zr alloys in the last 10 years. The observed trend in the number of published papers indicates a consistent upward trajectory, with the recent three years maintaining a count exceeding 600 papers. This observation underscores the significance of Zr alloys as a focal point within the broader field of materials science.

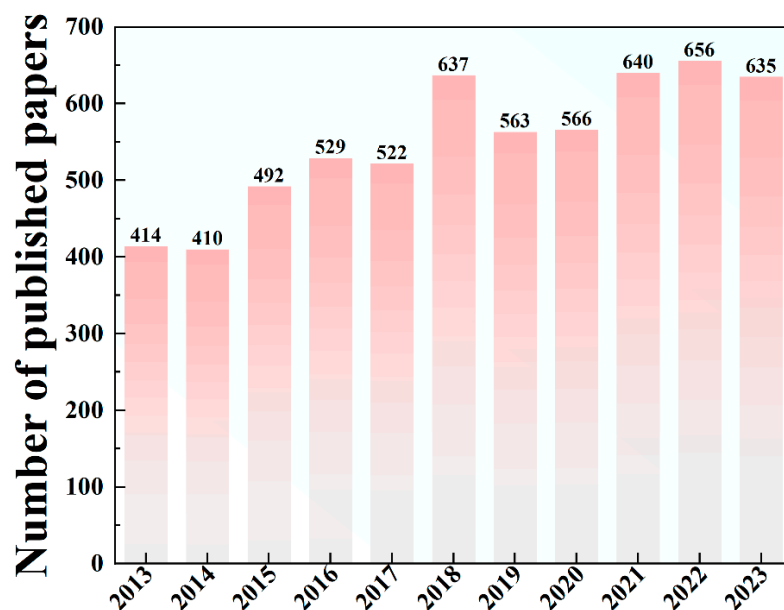


**Figure 1.** Number of publications published on Zr alloys in the Web of Science Core Collection in the last 10 years.

Furthermore, based on these bibliometric results, the research focus on Zr alloys was analyzed. Figure 2 depicts a network visualization of keywords that appear more



**Citation:** Dong, Q.; Tan, J. Advances in Zr-Based Alloys. *Crystals* **2024**, *14*, 351. <https://doi.org/10.3390/cryst14040351>

Received: 25 March 2024

Accepted: 29 March 2024

Published: 7 April 2024



**Copyright:** © 2024 by the authors. Licensee MDPI, Basel, Switzerland. This article is an open access article distributed under the terms and conditions of the Creative Commons Attribution (CC BY) license (<https://creativecommons.org/licenses/by/4.0/>).

than 40 times in papers related to Zr alloys over the last decade. The size of each circle corresponds to the frequency of keyword usage. Notably, prominent keywords such as “microstructure”, “corrosion”, “mechanical properties”, “oxidation”, “TEM”, “Ti”, “coating”, “ZrO<sub>2</sub>”, “hardness”, “phase transformation”, “SEM”, “texture”, “hydride”, “Hydrogen”, and “wear” rank among the top fifteen, signifying their central importance in the study of Zr alloys. Similarly, the colors of the circles indicate the relevance of the keywords, with each color representing a different cluster that may represent a given research direction. According to the color clustering of the keywords in Figure 2, several research directions on Zr alloys in recent years can be roughly summarized: (1) Research on the microstructure and mechanical properties of Zr alloys. (2) Research on the corrosion, wear, and protection of Zr alloys. (3) The oxidation and surface engineering of these alloys. (4) The characterization of recrystallization, texture, twinning, etc. (5). Experimental and computational simulations of phase transformation, precipitation behavior, and failure caused by hydrogenation, irradiation, creep, etc.

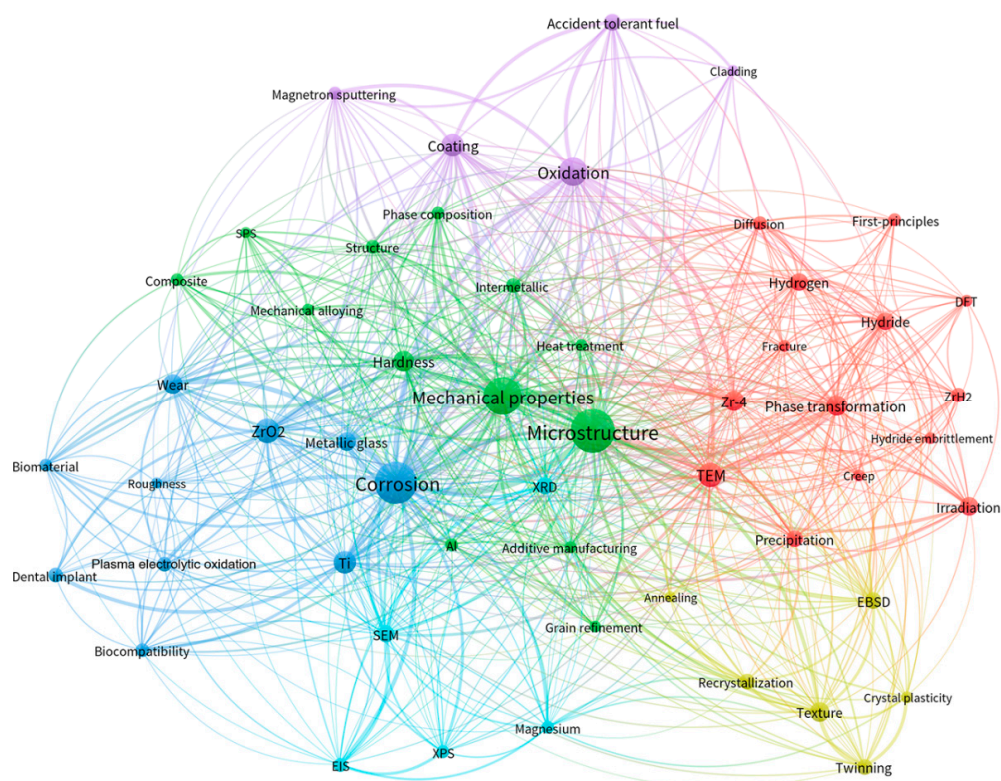


**Figure 2.** Network visualization of different keywords appearing no less than 40 times in the literature related to the term “Zirconium alloy” as published in the Web of Science Core Collection in the last 10 years.

Mechanical properties are one of the basic performance requirements of Zr alloys as a structural material, and the alloying [21–26] and processing [21,26–28] (including rolling, heat treatment, etc.) of Zr are extremely effective methods for modulating the material’s microstructure and improving its mechanical properties. The effect of Al content on the Zr’s mechanical properties and strengthening mechanisms has been thoroughly investigated by Wu et al. [29]. Al addition leads to grain size reduction and a Zr<sub>5</sub>Co<sub>7</sub>Al<sub>3</sub> intermetallic precipitation, and the best combination of mechanical properties (UTS and UFS of 464 MPa and 3.4%, respectively) was achieved for Zr<sub>47.5</sub>Co<sub>47.5</sub>Al<sub>5</sub> which demonstrated strong synergistic effects of fine grain strengthening, the solid-solution-strengthening of Al elements, and secondary-phase precipitation strengthening. Liu et al. [30] improved the mechanical properties of the new Zr-Ti-8V alloy through hot-rolling and annealing treatments and examined the effects of annealing temperatures. The phase composition

and mechanical properties of the rolled Zr-Ti-8V alloy were sensitive to the annealing temperature, i.e., many more fine needle-like  $\alpha$  phases were precipitated after annealing at 450 °C and the alloy exhibited the best strength–plastic ratio (1039 MPa, 8.2%). The dual-phase alloy with  $\alpha+\beta$  had higher hardness and wear resistance; however, the opposite trend was observed for the single  $\beta$ -phase alloy. Furthermore, the anisotropic mechanical behavior and associated microstructure evolution in annealed Zr-4 were investigated at room temperature by Sun et al. [31]. The basal  $\langle a \rangle$  slips were activated in the N ( $40^\circ$ – $50^\circ$ ) TB and TB orientation grains when loading along the RD, and the second-order pyramidal slips were activated in the grains when loading along the TD, leading to the anisotropic mechanical behavior of Zr-4 alloy.

The oxidation and microstructure stability of these alloys at high temperatures are the two main issues for their high-temperature applications. Surface modification technology is considered an effective means to improve the oxidation resistance of Zr alloys [32–36]. Wen et al. [37] investigated the oxidation behavior of FeCoNiCrMo high-entropy coatings by atmospheric plasma spraying on Zr-4 in steam at 1100 °C. A dense  $\text{Cr}_2\text{O}_3$  oxide layer was formed on the coating's surface after oxidation at 1100 °C, which grew from 1.5 to 3  $\mu\text{m}$  after 15 to 60 min of oxidation, and the FeCoNiCrMo high-entropy coatings and the substrates diffused simultaneously, the FeCoNiCrMo high-entropy coating can effectively delay the oxidation of the Zr-4 substrate. Zahra et al. [38] investigated the phase equilibria in the Ti-Al-Zr system at 1000–1300 °C via experimentation. The phase equilibria at all temperatures are different from the ones established before, i.e., B2-ordered  $\beta_0$  already exists at 1000 °C and remains stable up to at least 1300 °C and only traces of  $\text{Zr}_5\text{Al}_3$  were observed. The phase equilibria between  $\beta$ -Ti, Zr/ $\beta_0$ , TiAl, and  $\text{ZrAl}_2$  were determined at all temperatures.

Computer simulation of the irradiation effect in nuclear material is an important method for understanding its performance [39–43]. Pan et al. [44] investigated the trapping capability of small-vacancy clusters (two/three vacancies, V2/V3) in the  $\alpha$ -Zr doped with alloying elements (Sn, Fe, Cr, and Nb) via first-principle calculations. The alloying elements of Sn and Nb in the second site and Cr in the first site are more easily trapped by two vacancies in the supercells of  $\alpha$ -Zr containing 142-Zr atoms, respectively. The alloying elements of Sn in the third vacant site, Fe in the first vacant site, and Cr and Nb in the second vacant site are more easily trapped by three vacancies in the supercells of  $\alpha$ -Zr containing 141-Zr atoms, respectively.

Zirconia-based materials are widely used in nuclear energy engineering, engines, the biomedical field, power industries, etc., due to their outstanding chemical and radiation stability, as well as remarkable mechanical properties, such as high hardness, high strength, high fracture toughness, wear resistance, etc. [45–49]. Furthermore, the type and concentration of stable oxides significantly impact the structure, phase composition, and mechanical properties of some partially stabilized zirconia single crystals. Borik et al. [50] studied the phase composition, local structure, and mechanical characteristics of  $\text{ZrO}_2$  crystals partially stabilized with  $\text{Y}_2\text{O}_3$  and co-doped with  $\text{Nd}_2\text{O}_3$ ,  $\text{CeO}_2$ ,  $\text{Er}_2\text{O}_3$ ,  $\text{Tb}_2\text{O}_3$ , and  $\text{Yb}_2\text{O}_3$ . The phase composition and structure of crystals at the same total concentration of doping oxides depends on the degree of substitution of  $\text{Y}^{3+}$  cations by rare-earth cations, and the rare earth ions of the beginning of the lanthanide series predominantly occupy positions in the non-transformable tetragonal phase of crystals based on zirconium dioxide. The fracture toughness increases with an increase in the ionic radius of the rare earth element of the co-doped oxide, while the microhardness values of the crystals slightly decrease.

The present Special Issue on “Advances in Zr-Based Alloys” can be considered a status report reviewing the progress in Zr-based alloys that has been achieved over the past several years.

**Author Contributions:** All authors have read and agreed to the published version of the manuscript.

**Conflicts of Interest:** The authors declare no conflict of interest.

## References

1. Li, C.; Tan, J.; Zhu, X.; Zhang, Y.; Stoica, M.; Kühn, U.; Eckert, J. On the transformation-induced work-hardening behavior of Zr<sub>47.5</sub>Co<sub>47.5</sub>Al<sub>5</sub> ultrafine-grained alloy. *Intermetallics* **2013**, *35*, 116–119. [[CrossRef](#)]
2. Li, C.; Tan, J.; Wang, G.; Bednarčík, J.; Zhu, X.; Zhang, Y.; Stoica, M.; Kühn, U.; Eckert, J. Enhanced strength and transformation-induced plasticity in rapidly solidified Zr–Co–(Al) alloys. *Scr. Mater.* **2013**, *68*, 897–900. [[CrossRef](#)]
3. Zhong, L.; Feng, Z.; Zhao, S.; Tan, J.; Li, C.; Yi, J.; Eckert, J. Effect of stacking fault energy on B2 ZrCo phase transition and nanotwins formation in Zr<sub>54.5</sub>Co<sub>33.5</sub>Al<sub>12</sub> alloy prepared by rapid solidification. *Vacuum* **2024**, *221*, 112890. [[CrossRef](#)]
4. Zhou, Y.; Tian, W.; Dong, Q.; Wang, H.; Zhang, J.; Tan, J. First-principles calculations to investigate mechanical, electronic, optical, and thermodynamic properties of Zr-based ternary compounds. *J. Mater. Res. Technol.* **2023**, *23*, 1417–1434. [[CrossRef](#)]
5. Wang, H.; Zhou, Y.; Dai, L.; Mi, X.; Sun, C.; Dong, Q.; Wu, L.; Tan, J.; Tang, A. Interaction of displacement cascades with {10–12} and {10–11} twin boundaries in zirconium: A molecular dynamic study. *J. Mater. Res. Technol.* **2023**, *27*, 3362–3373. [[CrossRef](#)]
6. Wang, H.; Qin, C.; Zhou, Y.; Mi, X.; Wang, Y.; Kang, J.; Pan, R.; Wu, L.; She, J.; Tan, J.; et al. Interaction between collision cascades and nanocrack in hcp zirconium by molecular dynamics simulations. *Comput. Mater. Sci.* **2022**, *214*, 111688. [[CrossRef](#)]
7. Duan, Z.; Yang, H.; Satoh, Y.; Murakami, K.; Kano, S.; Zhao, Z.; Shen, J.; Abe, H. Current status of materials development of nuclear fuel cladding tubes for light water reactors. *Nucl. Eng. Des.* **2017**, *316*, 131–150. [[CrossRef](#)]
8. Azevedo, C. Selection of fuel cladding material for nuclear fission reactors. *Eng. Fail. Anal.* **2011**, *18*, 1943–1962. [[CrossRef](#)]
9. Yan, C.; Wang, R.; Wang, Y.; Wang, X.; Bai, G. Effects of ion irradiation on microstructure and properties of zirconium alloys—A review. *Nucl. Eng. Technol.* **2015**, *47*, 323–331. [[CrossRef](#)]
10. Stoll, U.; Slavinskaya, N. Corrosion behavior of zirconium alloys in the aqueous environment. Phenomenological aspects. Overview. *J. Nucl. Sci. Technol.* **2023**, *60*, 573–602. [[CrossRef](#)]
11. Kautz, E.; Gwalani, B.; Yu, Z.; Varga, T.; Geelhood, K.; Devaraj, A.; Senor, D. Investigating zirconium alloy corrosion with advanced experimental techniques: A review. *J. Nucl. Mater.* **2023**, *585*, 154586. [[CrossRef](#)]
12. Jiang, G.; Xu, D.; Yang, W.; Liu, L.; Zhi, Y.; Yang, J. High-temperature corrosion of Zr–Nb alloy for nuclear structural materials. *Prog. Nucl. Energy* **2022**, *154*, 104490. [[CrossRef](#)]
13. Jiang, G.; Xu, D.; Liu, J.; Yang, J.; Li, Y.; Kuang, W. Corrosion protection and failure mechanism of ZrO<sub>2</sub> coating on zirconium alloy Zry-4 under varied LiOH concentrations in lithiated water at 360 °C/18.5 MPa. *Appl. Surf. Sci.* **2023**, *650*, 159173. [[CrossRef](#)]
14. Zhang, Y.N.; Yang, H.L.; Juaim, A.N.; Chen, X.N.; Chang, L.U.; Ling, Z.O.U.; Wang, Y.Z.; Zhou, X.W. Biocompatibility and osteogenic activity of Zr–30Ta and Zr–25Ta–5Ti sintered alloys for dental and orthopedic implants. *Trans. Nonferrous Met. Soc. China* **2023**, *33*, 851–864. [[CrossRef](#)]
15. Tang, J.; Yang, H.; Qian, B.; Zheng, Y.; Vermaut, P.; Prima, F.; Sun, F. TWIP-assisted Zr alloys for medical applications: Design strategy, mechanical properties and first biocompatibility assessment. *J. Mater. Sci. Technol.* **2024**, *184*, 32–42. [[CrossRef](#)]
16. Byeli, A.; Kukareko, V.; Kononov, A. Titanium and zirconium based alloys modified by intensive plastic deformation and nitrogen ion implantation for biocompatible implants. *J. Mech. Behav. Biomed. Mater.* **2012**, *6*, 89–94. [[CrossRef](#)]
17. Adamson, R.B.; Coleman, C.E.; Griffiths, M. Irradiation creep and growth of zirconium alloys: A critical review. *J. Nucl. Mater.* **2019**, *521*, 167–244. [[CrossRef](#)]
18. Yang, Y.; Xiong, X.; Chen, J.; Peng, X.; Chen, D.; Pan, F. Research advances in magnesium and magnesium alloys worldwide in 2020. *J. Magnes. Alloys* **2021**, *9*, 705–747. [[CrossRef](#)]
19. Song, J.; Chen, J.; Xiong, X.; Peng, X.; Chen, D.; Pan, F. Research advances of magnesium and magnesium alloys worldwide in 2021. *J. Magnes. Alloys* **2022**, *10*, 863–898. [[CrossRef](#)]
20. Yang, Y.; Xiong, X.; Chen, J.; Peng, X.; Chen, D.; Pan, F. Research advances of magnesium and magnesium alloys worldwide in 2022. *J. Magnes. Alloys* **2023**, *11*, 2611–2654. [[CrossRef](#)]
21. Yan, J.; Wang, X.; Wang, Q.; Sun, X. Novel MRI-compatible Zr–Mo–Nb alloys with superior mechanical performance, high corrosion resistance and good cytocompatibility for biomedical applications. *J. Mater. Res. Technol.* **2024**, *30*, 794–806. [[CrossRef](#)]
22. Suyalatu; Kondo, R.; Tsutsumi, Y.; Doi, H.; Nomura, N.; Hanawa, T. Effects of phase constitution on magnetic susceptibility and mechanical properties of Zr-rich Zr–Mo alloys. *Acta Biomater.* **2011**, *7*, 4259–4266. [[CrossRef](#)]
23. Kondo, R.; Nomura, N.; Suyalatu; Tsutsumi, Y.; Doi, H.; Hanawa, T. Microstructure and mechanical properties of as-cast Zr–Nb alloys. *Acta Biomater.* **2011**, *7*, 4278–4284. [[CrossRef](#)]
24. Nie, L.; Zhan, Y.; Liu, H.; Tang, C. In situ synthesized low modulus biomedical Zr-4Cu-xNb alloys. *Mater. Sci. Eng. C* **2013**, *33*, 5105–5108. [[CrossRef](#)]
25. Zhan, Y.; Li, C.; Jiang, W.  $\beta$ -type Ti-10Mo-1.25Si-xZr biomaterials for applications in hard tissue replacements. *Mater. Sci. Eng. C* **2012**, *32*, 1664–1668. [[CrossRef](#)]
26. Zhang, X.; Zhang, B.; Liu, S.; Xia, C.; Ma, M.; Liu, R. Microstructures and mechanical properties of Zr–Al binary alloys processed by hot-rolling. *Mater. Sci. Eng. A* **2020**, *773*, 138723. [[CrossRef](#)]
27. Sun, X.; Liu, D.; Zhou, W.; Nomura, N.; Doi, H.; Tsutsumi, Y.; Hanawa, T. Effects of quenching process on microstructure, mechanical properties and magnetic susceptibility in Zr 1Mo alloy fabricated by powder bed fusion process. *Mater. Des.* **2020**, *187*, 108356. [[CrossRef](#)]
28. Wang, K.; Yin, R.; Xu, X.; Wei, W.; Tian, Y.; Deng, Z.; Zhang, L.; Liu, L. A study of mechanical and magnetic properties in a metastable Zr–10Nb–6Sn alloy for MRI-compatible hard tissue replacements. *J. Mater. Res. Technol.* **2024**, *29*, 2959–2970. [[CrossRef](#)]

29. Wu, Z.; Lu, W.; Li, C.; Gao, P.; You, X.; Tan, J. Effect of Al Content on the Microstructure and Tensile Properties of Zr-Co-Al Alloy Prepared by Rapid Solidification. *Crystals* **2022**, *12*, 1483. [[CrossRef](#)]
30. Liu, Y.; Chen, K.; Song, T.; Chen, B.; Li, Q.; Xia, C. Improvement of Mechanical Properties for a Novel Zr–Ti–V Alloy via Hot-Rolling and Annealing Treatment. *Crystals* **2022**, *12*, 1765. [[CrossRef](#)]
31. Sun, H.; Zhang, Y.; Sun, C.; Li, B.; Zhu, X.; Sun, Y.; Luan, B. Quasi-In Situ EBSD Study of Anisotropic Mechanical Behavior and Associated Microstructure Evolution in Zircaloy-4. *Crystals* **2022**, *12*, 1489. [[CrossRef](#)]
32. Syrtanov, M.; Kashkarov, E.; Abdulmenova, A.; Sidelev, D. High-temperature oxidation of Zr 1Nb zirconium alloy with protective Cr/Mo coating. *Surf. Coat. Technol.* **2022**, *439*, 128459. [[CrossRef](#)]
33. Kashkarov, E.; Sidelev, D.; Pushilina, N.; Yang, J.; Tang, C.; Steinbrueck, M. Influence of coating parameters on oxidation behavior of Cr-coated zirconium alloy for accident tolerant fuel claddings. *Corros. Sci.* **2022**, *203*, 110359. [[CrossRef](#)]
34. Kuprin, A.S.; Belous, V.A.; Voyevodin, V.N.; Bryk, V.V.; Vasilenko, R.L.; Ovcharenko, V.D.; Reshetnyak, E.N.; Tolmachova, G.N.; V'Yugov, P.N. Vacuum-arc chromium-based coatings for protection of zirconium alloys from the high-temperature oxidation in air. *J. Nucl. Mater.* **2015**, *465*, 400–406. [[CrossRef](#)]
35. Zhu, H.; Liu, H.; Zhou, J.; Dong, Y.; Li, P.; Chen, L.; Yi, J.; Huang, Q.; Huang, F.; Ge, F. Long-term oxidation resistance and deterioration mechanism of magnetron sputtered Cr-Al-Si-N coatings on zirconium alloys in 1200 °C steam atmosphere. *Corros. Sci.* **2020**, *171*, 108603. [[CrossRef](#)]
36. Brachet, J.-C.; Idarraga-Trujillo, I.; Le Flem, M.; Le Saux, M.; Vandenberghe, V.; Urvoy, S.; Rouesne, E.; Guilbert, T.; Toffolon-Masclat, C.; Tupin, M.; et al. Early studies on Cr-Coated Zircaloy-4 as enhanced accident tolerant nuclear fuel claddings for light water reactors. *J. Nucl. Mater.* **2019**, *517*, 268–285. [[CrossRef](#)]
37. Wen, L.; Li, Q.; Yang, B.; Yang, Z.; Wang, J.; Song, P. Oxidation Behavior of FeCoNiCrMo High-Entropy Coatings by Atmospheric Plasma Spraying on Zircaloy-4 in Steam at 1100 °C. *Crystals* **2022**, *12*, 1529. [[CrossRef](#)]
38. Kahrobaee, Z.; Rashkova, B.; Hauschildt, K.; Palm, M. Experimental Investigation of Phase Equilibria in the Ti–Al–Zr System at 1000–1300 °C. *Crystals* **2022**, *12*, 1184. [[CrossRef](#)]
39. Kong, X.; Wang, Q.; Yu, Y.; Shen, Y.; Zhang, C.; Pan, R.; Kharchenko, D.O.; Mao, J.; Ning, Z.; Fang, Z.; et al. Effect of solute Nb and Sn on self-interstitial atom defect in zirconium-based alloys by first-principles calculations. *J. Nucl. Mater.* **2024**, *588*, 154795. [[CrossRef](#)]
40. Christensen, M.; Wolf, W.; Freeman, C.; Wimmer, E.; Adamson, R.; Hallstadius, L.; Cantonwine, P.; Mader, E. Effect of alloying elements on the properties of Zr and the Zr–H system. *J. Nucl. Mater.* **2014**, *445*, 241–250. [[CrossRef](#)]
41. Samolyuk, G.; Barashev, A.; Golubov, S.; Osetsky, Y.; Stoller, R. Analysis of the anisotropy of point defect diffusion in hcp Zr. *Acta Mater.* **2014**, *78*, 173–180. [[CrossRef](#)]
42. Dai, C.; Saidi, P.; Yao, Z.; Daymond, M.R. Atomistic simulations of Ni segregation to irradiation induced dislocation loops in Zr–Ni alloys. *Acta Mater.* **2017**, *140*, 56–66. [[CrossRef](#)]
43. Wu, L.; Kharchenko, V.O.; Kong, X.; Kharchenko, D.O. First-principle calculations of vacancy clustering in zirconium-based alloys. *J. Nucl. Mater.* **2021**, *554*, 153079. [[CrossRef](#)]
44. Pan, R.; Tang, A.; Qin, J.; Xin, T.; Wu, X.; Wen, B.; Wu, L. Trapping Capability of Small Vacancy Clusters in the  $\alpha$ -Zr Doped with Alloying Elements: A First-Principles Study. *Crystals* **2022**, *12*, 997. [[CrossRef](#)]
45. Borik, M.A.; Kulebyakin, A.V.; Myzina, V.A.; Lomonova, E.E.; Milovich, F.O.; Ryabochkina, P.A.; Sidorova, N.V.; Shulga, N.Y.; Tabachkova, N.Y. Mechanical characteristics, structure, and phase stability of tetragonal crystals of ZrO<sub>2</sub>–Y<sub>2</sub>O<sub>3</sub> solid solutions doped with cerium and neodymium oxides. *J. Phys. Chem. Solids* **2021**, *150*, 109808. [[CrossRef](#)]
46. Han, J.; Göksel, B.; Li, M.; Vleugels, J.; Braem, A.; Castagne, S. Effects of femtosecond laser surface texturing on mechanical properties and low temperature degradation of alumina toughened zirconia. *J. Eur. Ceram. Soc.* **2024**, *44*, 4196–4209. [[CrossRef](#)]
47. Pereira, R.M.; Campos, T.M.B.; Bonfante, E.A.; Thim, G.P. A comparative study of mechanical properties of yttria stabilized zirconia monolithic and bilayer configuration for dental application. *J. Mech. Behav. Biomed. Mater.* **2023**, *148*, 106160. [[CrossRef](#)]
48. Kohal, R.; Wolkewitz, M.; Mueller, C. Alumina-reinforced zirconia implants: Survival rate and fracture strength in a masticatory simulation trial. *Clin. Oral Implants Res.* **2010**, *21*, 1345–1352. [[CrossRef](#)]
49. Schierano, G.; Mussano, F.; Faga, M.G.; Menicucci, G.; Manzella, C.; Sabione, C.; Genova, T.; von Degerfeld, M.M.; Peirone, B.; Cassenti, A.; et al. An Alumina Toughened Zirconia Composite for Dental Implant Application: In Vivo Animal Results. *BioMed Res. Int.* **2015**, *2015*, 157360. [[CrossRef](#)]
50. Borik, M.A.; Kulebyakin, A.V.; Lomonova, E.E.; Milovich, F.O.; Myzina, V.A.; Ryabochkina, P.A.; Tabachkova, N.Y.; Sidorova, N.V.; Chislov, A.S. Partially Yttria-Stabilized Zirconia Crystals Co-Doped with Neodymium, Cerium, Terbium, Erbium or Ytterbium Oxides. *Crystals* **2021**, *11*, 1587. [[CrossRef](#)]

**Disclaimer/Publisher's Note:** The statements, opinions and data contained in all publications are solely those of the individual author(s) and contributor(s) and not of MDPI and/or the editor(s). MDPI and/or the editor(s) disclaim responsibility for any injury to people or property resulting from any ideas, methods, instructions or products referred to in the content.